Theor Chem Acc (2006) 116: 711–717
DOI 10.1007/s00214-006-0117-1

REGULAR ARTICLE

Michele Pavanello · Benedetta Mennucci · Jacopo Tomasi

DFT calculation of deuterium quadrupolar tensor in crystal anthracene

Received: 28 November 2004 / Accepted: 07 January 2005 / Published online: 21 February 2006

Abstract A DFT calculation of deuterium nuclear quadrupole tensors of crystal anthracene is presented. After a careful analysis of the DFT functionals and of the basis sets, the B3LYP/6-311+G(d,3p2d) level has been identified as the best compromise between accuracy and computational cost. To account for the crystal environment, three models are proposed: one represented by a cluster of five anthracene arranged as in the crystal, the other formed by an anthracene embedded in a dielectric continuum having the dielectric permittivity of the crystal, and the last represented by an embedded dimer of anthracene. It is shown that the pure continuum model (here represented by the Integral Equation Formalism version of the Polarizable Continuum Model) already accounts for a large part of the crystal effects and that the embedded dimer almost entirely recover all the details of the explicit 5-anthracene cluster.

1 Introduction

The coupling between the nuclear quadrupole moment and the electric-field-gradient tensor is, besides the Zeeman effect, the most important interaction of nuclear spins (≥ 1) with their environment. Since this coupling depends strongly on the electronic environment of the nucleus, nuclear quadrupole coupling tensors (QCTs) are one of one-electron molecular quantities mostly used as a probe of the electronic distribution in molecules.

The QCTs are of interest for a number of different spectroscopies, for example molecular beam resonance spectroscopy, nuclear magnetic resonance (NMR) [1], nuclear quadrupole resonance (NQR) [2,3], Mössbauer spectroscopy [4,5], and also electron paramagnetic resonance (EPR) [6]. These techniques exploit specific nuclear characteristics (distinct isotopes, decay of excited nuclear states, nuclear spin transitions, etc.), which involve the coupling between the nuclear quadrupole moment and the electric field gradient (EFG) at the nucleus. More specifically, in the NMR, the QCT is commonly measured in crystal solids (solid-state NMR) [7] or in liquid crystalline compounds (LC-NMR) [8] to extract information on the structure and on the orientational order, respectively. In the LC-NMR, to get the orientational order parameters, it is necessary to know the QCTs expressed in a molecular fixed frame. It is rarely possible to get these QCTs experimentally. In fact, in the best cases, QCTs are taken from measurements on the same compounds in the solid-state or, more commonly, from other similar molecules. For example, most of the data of orientational order extracted from QCTs of aromatic systems dissolved in Liquid Crystals are derived using QCT values taken from Solid-State NMR of Anthracene [9]. Some investigations about possible deviations of QCTs of different aromatic substances from Anthracene have been reported [10–12] but a detailed electronic analysis, as through accurate Quantum-Mechanical (QM) approaches, is still missing.

The comparison of measured values of QCTs with QM electronic calculations can in fact represent an important strategy to study correlations between electronic distributions and structure. From a theoretical point of view, QCTs are proportional to the electric nuclear quadrupole moment (NQM) of the nucleus and the EFG at that nucleus, and the EFG gives valuable information about the electron distribution surrounding the nucleus. Due to this sensitivity, the QCT, and in particular, the EFG of open shell atoms and small closed shell molecules have been studied using highly correlated ab initio calculations [13–20], and, more recently, also fully relativistic all-electron (correlated) methods [21,22]. An alternative to ab initio calculations is the use of density functional theory (DFT), since for many properties it can provide accurate results at a low computational cost. Starting from 1997, DFT has been largely and successfully applied to the calculation of EFG [23–33]. The present paper is a further example of the applicability of DFT to the determination of QCT but, with respect to previous papers on this subject, here the interest is focused not on the definition of

M. Pavanello · B. Mennucci (✉) · J. Tomasi
Dipartimento di Chimica e Chimica Industriale, via Risorgimento 35, 56126 Pisa, Italy
E-mail: bene@dcci.unipi.it
E-mail: tomasi@dcci.unipi.it

the most appropriate combination of functional and basis set (even if a study on these effects are also reported) but on the consideration of environmental effects. The interest here is in fact the comparison of calculated QCT of anthracene with the experimental value measured in the crystal. To account for the crystalline environment two models are compared, one based on the real 3D structure of the crystal, and the second based on a dielectric continuum description using the dielectric permittivity of the crystal. In the present paper, the dielectric continuum approach is based on the Integral Equation Formalism (IEF) [34–36] version of the Polarizable Continuum Model (PCM) [37,38]. In its standard formulation, PCM is a model to describe molecular solutes immersed in isotropic solutions by using a molecular-shaped cavity to define the boundary between solute and continuum dielectric, and apparent surface charges mimicking the electrostatic solvent effects. In the IEF reformulation, the PCM approach has been generalized to treat more complex environments like ionic solutions and anisotropic dielectrics (namely liquid crystals or crystalline solids). In parallel, extensions to quantum-mechanical approaches to evaluate environmental effects on molecular properties have been also presented [39]. In the present paper the IEFPCM approach is used to evaluate the quadrupolar coupling tensor of anthracene when in the solid phase.

The paper is organized as follows: in sect. 2 a brief summary of the theoretical aspects of the definition and the calculation of QCT is reported; in sect. 3 the analysis of both QM aspects and environmental effect on the QCT of anthracene is described and finally in sect. 4 some comments and suggestions of further investigation are given.

2 Theoretical background

As reported in the Introduction, the EFG at a nucleus A will, for a nucleus with spin larger or equal to 1, interact with the electric nuclear quadrupole moment to produce a coupling characteristic of that nucleus in that specific molecule. The EFG tensor, $\mathbf{V}$, whose components $V_{\alpha,\beta}(A)$ are defined as the derivatives of the electric field component α with respect to the coordinate β, is a symmetric and real tensor. It thus exists a coordinate system, known as Principal Axis System (PAS), with respect to which $\mathbf{V}$ is diagonal. In addition, $\mathbf{V}$ is traceless and thus, there will be only two independent terms. As a result, also the QCT will be diagonal, and univocally described in terms of two terms, the nuclear quadrupole coupling constant (qcc), $q_{zz}(A)$, and the asymmetry parameter, $\eta(A)$,

$$q_{zz}(A) = \frac{eQ(A)}{h} V_{zz}(A),$$
$$\eta(A) = \frac{q_{yy}(A) - q_{xx}(A)}{q_{zz}(A)} = \frac{V_{yy}(A) - V_{xx}(A)}{V_{zz}(A)}, \qquad (1)$$

where $Q(A)$ is the electric quadrupole moment of the nucleus A, e the proton charge, h the Plank's constant, and $V_{\alpha,\beta}(A)$ are the EFG Cartesian components at the site of the nucleus A. In particular, the PAS for the EFG tensor is chosen such that $|V_{zz}| \geq |V_{yy}| \geq |V_{xx}|$, whereby $0 \leq \eta \leq 1$.

2.1 QM definition of the EFG

The EFG arises from other nuclei in the molecule and from the electronic charge distribution. The zz component due to the i-th electron at a point which is at a distance r_{iA} from the nucleus A at an angle θ_{iA} with respect to the z axis can be shown to be [1]:

$$V_{zz} = e\left(\frac{3\cos^2\theta_{iA} - 1}{r_{iA}^3}\right) \qquad (2)$$

The total zz component of the EFG in a molecule, composed by N nuclei, at the site of the nucleus A is then

$$\langle V_{zz}(A)\rangle = e\sum_{K\neq A} Z_K \frac{3\cos^2\theta_{KA} - 1}{R_{KA}^3} - e\left\langle \Phi \left| \sum_i \frac{3\cos^2\theta_{iA} - 1}{r_{iA}^3} \right| \Phi \right\rangle \qquad (3)$$

where Φ is the electronic ground-state wavefunction, and the first summation is over all the nuclei in the molecule different from A. It is evident from Eq. (3) that charges close to the nucleus will have a much greater influence on the total field gradient than charges that are more distant. Thus, the magnitude of the field gradient will strongly depend on the chosen basis functions of the nucleus in analysis. For example, in the past, QCTs were used as an indication of the amount of p character in the s–p hybrid bond involved [40].

Being a simple electronic expectation value (3), one would expect that an accurate calculation of EFGs is a simple task. However, the r_{iA}^{-3} dependency of the electronic EFG operator as opposed to the r_{iA}^{-1} potential in the usual molecular Hamiltonian together with its angular dependence makes the calculation not completely trivial. An interesting observation that comes from Eq. (3) is that s functions does not give contribution to the EFG because of their spherical symmetry, so we can infer from now that polarization functions are of great importance in the choice of the basis set.

2.2 Determination of deuterium quadrupole moment

In the past years a large attention has been paid at the accurate determination of the QCTs, especially for the deuterium nucleus, for which there is a quite large literature [41–46]. In order to apply QM calculations of EFG to the study of deuterium QCT of molecular systems of interest, it is necessary to have an accurate value of the deuterium quadrupole moment Q. The method followed to get this value was first to get a precise NMR measurement of the deuterium quadrupole coupling tensor of small molecules as HD or D_2 for which very accurate QM calculations of EFG can be performed, and then extract the deuterium quadrupole moment Q by means of Eq. (1).

This procedure has been applied to D_2 for which the deuterium quadrupolar splitting has been measured with large accuracy by Code and Ramsey [41], and the EFG, V_D, has

been obtained by Bishop and Cheung [43] through a nonadiabatic calculation using a wavefuntion explicitly containing the vibronic component ($\langle V_{\mathrm{D}} \rangle = 0.33466\ a.u$).

By introducing the experimental value of q_{D} and the calculated one of the EFG, from Eq. (1) we get:

$$Q = \frac{q_D}{\langle V_D \rangle} = \frac{225.044}{0.33466} = 672.456 \text{ KHz/au} \quad (4)$$

which is, at present, the most accurate value for the deuterium quadrupole moment (the uncertainty on q_{D} is of ± 0.024 KHz). This is exactly the value used for Q in the present paper.

3 The study of the QCT in anthracene

3.1 Theory level analysis

As reported in the Introduction, many QM methods have been used to describe the EFG. Among them, here we shall consider the DFT approach. In the last years DFT methods have been successfully applied to the study of many molecular properties using many different functionals. However, there is a particular hybrid functional which has been shown to be accurate for many different kinds of calculations and thus it has become one of the most used, namely the Becke- three parameter Lee-Yang-Parr functional (B3LYP) [47]. A previous study [13][e] has shown that B3LYP correctly reproduces deuterium QCTs in various small/medium molecules: to verify if this reliability of B3LYP applies also for anthracene, we have done a preliminary comparison with three among the most widely used functionals. Namely we tested two pure functionals, BLYP (Becke's 1988 exchange functional, which includes the Slater exchange along with corrections involving the gradient of the density, and correlation functional of Lee, Yang, and Parr which includes both local and non-local terms [48,49]) and PBEPBE (exchange and gradient-corrected correlation functionals of Perdew, Burke and Ernzerhof [50–52]), and another hybrid functional, namely B3PW91 (same as B3-LYP but with the nonlocal correlation term of Perdew and Wang [53]). For comparison with DFT we also carried out Hartree-Fock (HF) and Møller-Plesset second-order (MP2) calculations. These calculations, as well as all the following ones, have been performed using the GAUSSIAN-03 [54] computational package.

To perform the test we have chosen a sufficiently large basis set including polarization functions on both heavy atoms and hydrogens, e.g. the 6-311+G(d,p) basis set, and we have computed q_{CD} and η for the different deuterium nuclei of anthracene using the various functionals. The results are reported in Table 1. We should mention that, for each level of calculation, a single value for q_{CD} and η has been reported, obtained as an average of the values of all deuterium nuclei; the corresponding experimental averaged values measured in the crystal are $q_{\mathrm{CD}} = 181 \pm 3$ KHz and $\eta = 0.064 \pm 0.013$ [9]. Here the $\pm$ does not indicate the uncertainty but the differences in the q_{CD} and η values for the various deuterium nuclei with respect to the mean values: the uncertainty on each principal component of the QCT is ± 3 KHz, this error propagates to gives a relative uncertainty of about 50% on the value of the experimental η.

Table 1 Average qcc and asymmetry parameter of Anthracene computed in vacuo at DFT, HF and MP2 levels

Level of theory	q_{CD}	η
B3LYP	209.609	0.0781
B3PW91	210.839	0.0753
BLYP	209.084	0.0761
PBEPBE	210.652	0.0724
HF	215.202	0.0885
MP2	215.752	0.0770

For DFT calculations, four different functionals have been tested. All calculations have been done using the 6-311+g(d,p) basis set

As we can see from Table 1, BLYP and B3LYP functionals seem to give better results for both q_{CD} and η with respect to the other functionals. It is also interesting to note, that MP2 corrections do not really improve the HF value for q_{CD} while they significantly reduce the asymmetry parameter, η. In any case, MP2 seems not to be competitive with DFT approaches, and in particular with the B3LYP functional. This result is not new; there are in fact previous works that observe the same behavior of the MP2 method also for other nuclei [55]. For these reasons, in the following, we thus shall limit the calculations at B3LYP level.

3.2 Basis set analysis

After defining the functional, we now proceed to analyze the effect of the basis set.

We have carried out the basis set analysis first by making a choice between the Pople style basis set and the correlation–consistent (cc) ones, see Table 2.

The first comment to make is that the two sets behave very differently when passing from double-zeta (DZ) to triple-zeta (TZ) type of basis sets: while in the cc class this change implies a significant improvement in the quality of the quadrupolar tensor (and this is shown both in the qcc and

Table 2 Average qcc and asymmetry parameter od anthracene calculated in vacuo at DFT(B3LYP) level with the geometry calculated at B3LYP/6-31+G(d) in vacuo

Basis	N[a]	$q_{CD}(KHz)$	η
cc-pVDZ	246	211.157	0.0657
aug-cc-pVDZ	412	209.375	0.0543
cc-pVTZ	560	193.322	0.0758
aug-cc-pVTZ	874	193.291	0.0760
6-31G(d,p)	260	200.864	0.0758
6-31+G(d,p)	316	200.646	0.0804
6-31++G(d,p)	326	200.653	0.0801
6-311G(d,p)	312	209.360	0.0777
6-311+G(d,p)	368	209.609	0.0781
6-311++G(d,p)	378	209.653	0.0780
6-311G(d,3pd)	422	193.991	0.0803
6-311+G(d,3pd)	478	193.816	0.0795
6-311++G(d,3pd)	488	193.991	0.0796

[a] Total number of basis functions

Table 3 Average qcc and asymmetry parameter of anthracene calculated in vacuo at DFT(B3LYP) level, with the geometry calculated at B3LYP/6-31+G(d) in vacuo

6-311+g(·, ·)	N	$q_{CD}(KHz)$	η
d,p	368	209.609	0.0781
d,2p	398	203.846	0.0827
d,3p	428	204.416	0.0819
2d,p	438	208.389	0.0669
2d,2p	468	202.885	0.0723
2d,3p	498	203.456	0.0709
3d,2p	538	204.436	0.0713
3d,3p	568	205.162	0.0718
3df,3p	666	199.895	0.0699
d,pd	418	195.168	0.0774
d,2pd	448	194.805	0.0786
d,3pd	478	193.816	0.0795
d,3p2d	528	186.437	0.0838
2d,3pd	548	194.654	0.0789
df,pd	516	195.089	0.0746
3df,3pd	726	194.179	0.0768

in the asymmetry), in the Pople class this improvement is not found. This finding is, however, not completely unexpected as it is well known that Pople basis sets cannot be used to generate a sequence which converges toward the basis limit while this can be done with the cc basis sets.

From the analysis of the results of Table 2, the DZ results will not be discussed any longer, and we will focus on the systematic trends exposed by the TZ basis sets and try to estimate basis set limits on the basis of these trends.

Both in the cc and in the Pople sets, it is evident that the presence of diffuse functions (either on carbons only or on both atoms) does not significantly increase the quality of the quadrupolar tensor: in the cc set, the change in q_{CD} is less than 0.5 KHz and almost null on the asymmetry parameter η; in the Pople set, the same change is always smaller than 0.2 KHz for q_{CD} and negligible for η starting either from 6-311G(d,p) or 6-311(d,3pd). By comparing cc and Pople sets results and the corresponding number of functions, it appears quite evident that the TZ Pople family (when properly supplemented with diffuse and polarization functions) represents the best choice in terms of quality of the results and gain in the computational efforts. However, before passing to study the real subject of our study, namely the environmental effects, a last analysis deserves to be done, namely the choice of the correct type and number of polarized basis functions on the hydrogens and on the carbons.

In Table 2 we have analyzed only two types of polarization functions, namely (d,p) and (d,3pd), in Table 3 we present a more systematic analysis starting from 6-311+G(d,p) and adding polarization functions on both carbons and hydrogens.

From Table 3 we can see that a central role is played by *d* functions on hydrogens while it is almost useless to enlarge the number of *d* functions on carbons, or adding *f* functions. A qualitative explanation of this behavior is that the smoother the description of the wavefunction around deuterium nuclei, the better the electric field gradient at the site of that nucleus (see sect. 2).

From the results reported in Tables 2 and 3, we can safely define the 6-311+G(d,3p2d) basis set as the best choice both in terms of quality and computational price and thus we shall perform the following analysis on the environmental effect using this basis set.

3.3 Effect of the environment

To study the effect of the crystal environment, we have defined two alternative strategies. We have first tried to reproduce the effects of the crystal, at least its electrostatic component, by using an embedded system, i.e. anthracene within a cavity inside a dielectric continuum characterized by a dielectric tensor with principal components equal to those measured in the crystal anthracene at 293 K, namely 2.42, 2.90, 4.07 [56]. Due to the very low anisotropy of this tensor, we have approximated the crystal with an isotropic dielectric having as permittivity constant the mean value of the three components of the tensor, namely $\varepsilon = 3.13$. As for any other molecular property, the effects of the embedding medium on the QCT are of two types: there is a direct effect on the electronic charge distribution and an indirect effect through variations induced in the molecular geometry. In order to quantify these two effects separately, we have done two different PCM calculations of the QCT for the embedded anthracene (at B3LYP/6-311+G(d,3p2d) level), the first using the geometry optimized for the isolated system (vac) and the second using the geometry optimized in this hypothetical dielectric medium (both obtained at B3LYP/6-31+G(d)).

In the Table 4, we show the values of q_{CD} and η of anthracene calculated in gas phase (vac) and in the continuum (PCM) using the two different molecular geometries. Due to symmetry reasons, three different deuteriums are present in the anthracene, their numeration is indicated in the Fig. 1.

Table 4 B3LYP76-311+G(d,3p2d) QCT of isolated and embedded anthracene

Method	vac		PCM		PCM	
Geometry	vac		vac		PCM	
deuteriums	$q_{CD}(KHz)$	η	$q_{CD}(KHz)$	η	$q_{CD}(KHz)$	η
1	186.968	0.0776	187.005	0.0785	186.320	0.0788
2	186.498	0.0820	185.480	0.0850	184.823	0.0852
3	185.845	0.0917	184.135	0.0943	183.536	0.0945

For the embedded system two sets of data are presented: those obtained using the gas-phase geometry (vac) and those obtained using the embedded geometry (PCM)

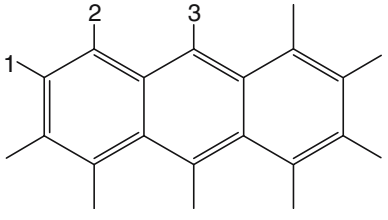

Fig. 1 Numeration used to identify the different deuteriums of anthracene

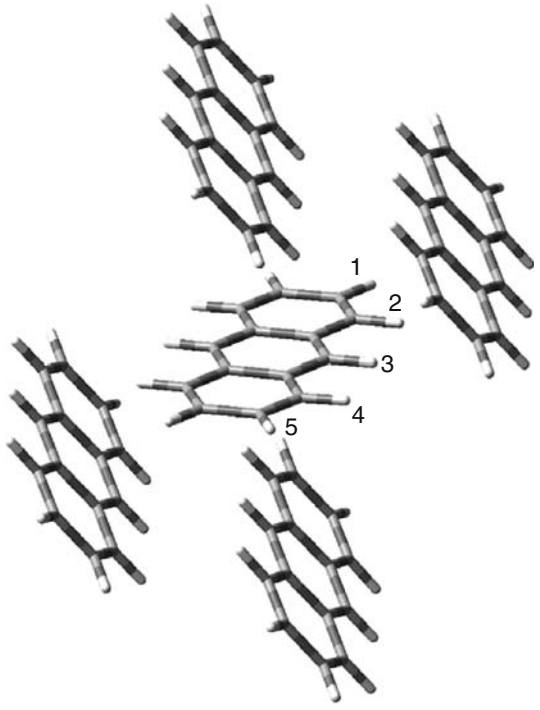

Fig. 2 Representation of the cluster of five anthracene molecules obtained from the X-ray structure of the unit cell [57–59]

Table 5 QCT of 5-anthracene cluster obtained from crystal anthracene at T=220K

Geometry	vac		PCM	
deuterium	$q_{CD}(KHz)$	η	$q_{CD}(KHz)$	η
1	186.177	0.0752	185.078	0.0755
2	182.382	0.0741	181.277	0.0744
3	183.857	0.0882	182.755	0.0886
4	186.264	0.0800	185.165	0.0804
5	187.437	0.0750	186.337	0.0753
<exp>	$q_{CD} = 181 \pm 3$		$\eta = 0.064 \pm 0.013$	

The calculated values have been obtained using a mixed basis set: 6-311+G(d,3p2d) for the inner fragment and 6-31+G(d) for the other four fragments. The two sets of data refer to two different CH bond lengths, namely R_{CH}=1.0875 (vac), and R_{CH}=1.0885 (PCM)

Table 6 B3LYP/6-311+G(d,3p2d) QCT of the embedded dimer of anthracene

Deuterium	$q_{CD}(KHZ)$	η
1	184.558	0.0782
2	181.388	0.0765
3	182.456	0.0902
4	184.700	0.0816
5	185.302	0.0801

By comparing the results reported in the left column with those in the two PCM columns, we can estimate the direct and the indirect environment effects. As regards q_{CD}, the direct effect (comparison of the two column using the same gas-phase geometry, columns "Geometry vac") increases, passing from D1 to D2 and D3; in particular, for the most "internal" D3 a decrease of around 2 KHz is found. Adding also the indirect effect due to the relaxed geometry (column "Geometry PCM") a further 0.6 KHz decrease is observed. The embedding effects on η are almost only of direct type as the relaxation of the geometry induces only a negligible change with respect to the unrelaxed system.

As alternative strategy, we can now explicitly consider the effects of the first neighbors of each anthracene molecule in the crystal by using the X-ray structure of the unit cell [57–59] and starting from this to build the proper cluster. The crystal is monoclinic (space group $C_{2h} - P2_1/a$) and the unit cell consists of two molecules; by using symmetry relations we have obtained a cluster of five anthracene molecules which is reported in Fig. 2.

Unfortunately, the X-ray structure cannot give information on the C-H bond lengths. To overcome this limitation we have resorted to quantum-mechanical calculations and used the CH bond lengths obtained in the B3LYP/6-31+G(d) optimizations described above. In particular, we have tested both bond lengths obtained in the gas-phase optimization and those obtained in the optimization of the embedded (PCM) system: in the former case we have an average CH bond length of $R_{\mathrm{CH}} = 1.0875$ Å. and in the latter case $R_{\mathrm{CH}} = 1.0885$.

Due to the large dimension of the cluster, to compute the quadrupolar tensor we have defined an hybrid approach using the large 6-311+G(d,3p2d) basis set for the central molecule and the smaller 6-31G for the other four anthracene molecules. The results of the QCT of the deuteriums in the central anthracene are reported in Table 5. Notice that in the 5-antracene cluster arrangement, five different deuteriums are present in the central anthracene: their numeration is shown in Fig. 2. We note that, because of the not symmetric arrangement, deuterium 1 and 5, and 2 and 4, are not equivalent; in particular, deuterium 2 is the one which is closest to the other anthracene molecule.

The results of the cluster with PCM-derive R_{CH} bond lengths are indeed very good: both the q_{CD} and the η are in fact correctly within the experimental range of values. This clearly shows that, when one wants to compare with experiments, besides a careful analysis of the level of calculation and of the basis set, it is also important to take into account possible effects due to the physical environment.

The comparison of the results reported in Table 5 for the 5-anthracene cluster and in Table 4 for the embedded anthracene seems to indicate that to correctly reproduce the QCT in the crystal, both the specific effects of the first neighbor and those of all the other molecules have to be included. A simple but efficient way to do this is to use an embedded dimer, i.e. to use the dimer of the unit cell and embed it in the continuum medium defined above. The graphical representation of the isolated and the embedded dimers are shown in Fig. 3 and the results of the quadrupolar tensor for the various deuteriums are reported in Table 6. Notice that for this calculation, we have used the CH bond length obtained from PCM geometry optimization, namely $R_{\mathrm{CH}} = 1.0885$ Å.

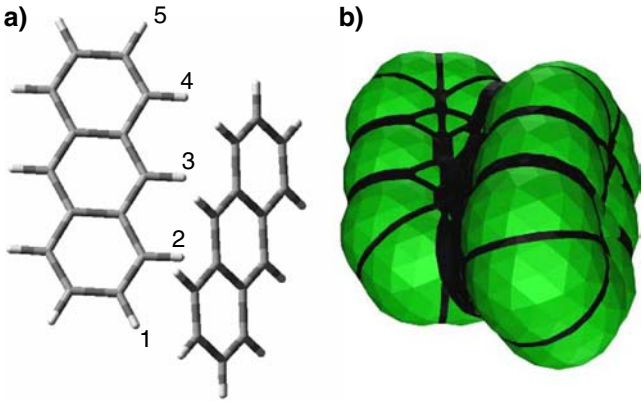

Fig. 3 Graphical representation of the isolated and the embedded dimer (i.e. the molecular cavity used in the IEFPCM calculation)

The results are indeed quite good when compared with those computed in the 5-anthracene cluster (Table 5): for all deuteriums, both q_{CD} and the asymmetry parameter η are in fact well reproduced by the embedded dimer.

This is an interesting result because it shows that a simplified system as those of a dimer embedded in a continuum dielectric correctly reproduce the effects of the 3D structure of a crystal. It is also interesting to note that the effects of the embedding alone (see Table 4), i. e. without explicitly considering intermolecular interactions, already captured the large part of the reduction observed passing from the isolated anthracene to the crystal.

4 Conclusions

A DFT calculation of deuterium QCT of solid anthracene is presented here. The accurate determination of deuterium QCTs of aromatic substances is important, especially in LC-NMR, as a wide number of liquid crystals rigid-cores are aromatic. As a typical aromatic probe, anthracene is commonly used and thus this work has been focused on it; however, in principle, the same computational strategy is transferable to any other kind of molecules.

The computational strategy followed to determine both qcc and asymmetry parameter of the various deuteriums in anthracene has been the following. After a careful choice of the proper functional and basis set, three alternative methods have been tested to account for the interactions between the molecule in analysis and its environment:

1. A single anthracene molecule embedded in a dielectric, with dielectric properties derived from the crystal anthracene, except for the dielectric anisotropy.
2. A five-anthracene cluster obtained from experimental crystal structure.
3. An embedded dimer, based on the geometry of crystal anthracene.

From the comparison of the results obtained using these three approaches, it is clear that a correct description of deuterium QCTs in crystal anthracene requires to introduce explicit intermolecular interactions, either through an expensive calculation on the large cluster or, more efficiently, by using a mixed continuum/discrete strategy, here represented by the embedded dimer. It is however interesting to point out that also a very simplified model as that represented by a single anthracene molecule surrounded by the continuum, already accounts for a large part of the crystal effects. These results lead us to conclude that the PCM method can represent a good model to take into account the environmental effects on the deuterium QCTs at low computational cost but still keeping a sufficient accuracy.

In addition, we note that, even if this work has been limited to deuterium QCT, many other nuclei are of large interest and could be analyzed with similar techniques. The only issue to take care of when other nuclei, such as for example ^{14}N or ^{17}O, are studied is that, due to the more complex electronic charge distribution, a reconsideration of the functional as well as of the basis set has to be done [14]. We note, however, that deuterium still remains an important nucleus to study as largely used, especially in LC-NMR, due to its well resolved spectra. The main goal of the present paper is thus that of suggesting a simple but accurate computational strategy to obtain deuterium QCTs of molecular systems not limited to few atoms, without requiring extremely high computational efforts. The next step will be in fact the generalization of the method to the study of orientational order in liquid crystals.

References

1. Slichter CP (1963) Principles of Magnetic Resonance (Harper and Row, New York)
2. Semin GK, Babushkina TA, Yakobson GG (1975) Nuclear quadrupole resonance in chemistry, Wiley, New York
3. EAC Lucken (1969) Nuclear quadrupole coupling constants Academic Press, New York
4. Gonser U (ed) (1975) Mössbauer spectroscopy Springer, Berlin Heidelberg New York
5. Greenwood N, Gibb TC (1971) Mössbauer spectroscopy Chapman and Hall, London
6. Weil JA, Bolton JR, Wertz JA (1994) Electron paramagnetic resonance: elementary theory and practical applications, Wiley, New York
7. Mehring M (1983) Principles of high resolution NMR in solids, Springer, Berlin Heidelberg New York
8. Burnell EE, de Lange CA (2003) NMR of ordered liquids, Kluwer Academic Publisher, Dordrecht
9. Ellis DM, Bjorkstam J (1967) J Chem Phys 46: 4460
10. Diehl P, Reinhold M (1978) Mol Phys 36: 143
11. Emsley JW, Longeri M (1981) Mol Phys 42: 315
12. Merlet D, Emsley JW, Jokisaari J, Kaski J (2001) Phys Chem Chem Phys, 3: 4918
13. Sundholm D, Olsen J (1993) J Chem Phys 98: 7152
14. Halkier A, Koch H, Christiansen O, Jørgensen P, Helgaker T (1997) J Chem Phys 107: 849
15. Tokman M, Sundholm D, Pyykkö P (1998) Chem Phys Lett 291: 414
16. Pernpointner M, Schwerdtfeger P (1998) Chem Phys Lett 295: 347
17. Pernpointner M, Seth M, Schwerdtfeger P (1998) J Chem Phys 108: 6722
18. Kellö V, Sadlej A (1999) J Mol Phys 96: 275
19. Kellö V, Sadlej AJ, Pyykkö P, Sundholm D, Tokman M (1999) Chem Phys Lett 304: 414

20. Olsen L, Christiansen O, Hemmingsen L, Sauer SPA, Mikkelsen KV (2002) J Chem Phys 116: 1424
21. Visscher L, Enevoldsen T, Saue T, Oddershede J (1998) J Chem Phys 109: 9677
22. de Jong WA, Visscher L, Nieuwpoort WC (1999) J Mol Struct 458: 41
23. Eriksson LA, Malkina OL, Malkin VG, Salahub DR (1997) Int J Quantum Chem 63: 575
24. Dufek P, Blaha P, Schwarz K (1998) Phys Rev Lett 75: 3545
25. Havlin RH, Godbout N, Salzmann R, Wojdelski M, Arnod W, Schulz CE, Oldfield E (1998) J Am Chem Soc 120: 3144
26. Godbout N, Havlin R, Salzmann R, Debrunner PG, Oldfield E (1998) J Phys Chem A, 102: 2342
27. Bailey WC (1997) J Mol Spectrosc 185: 403
28. Schwerdtfeger P, Pernpointner M, Laerdahl JK (1999) J Chem Phys 111: 3357
29. Lenthe Ev, Baerends EJ (2000) J Chem Phys 112: 8279
30. Alonso RE, Svane A, Rodriguez CO, Christensen NE (2004) Phys Rev B 69: 125101
31. Bailey WC (1998) Chem Phys Lett 292: 71
32. Bailey WC (2000) Chem Phys 252: 57
33. Fritscher J (2004) Phys Chem Chem Phys 6: 4950
34. Cancès E, Mennucci B (1998) J Math Chem 23: 309
35. Cancès E, Mennucci B, Tomasi J (1997) J Chem Phys 107: 3031
36. Mennucci B, Cancès E, Tomasi J (1997) J Phys Chem B 101: 10506
37. Miertus S, Scrocco E, Tomasi J (1981) Chem Phys 55: 117
38. Cammi R, Tomasi J (1995) J Comp Chem 16: 1449
39. Tomasi J, Cammi R, Mennucci B, Cappelli C, Corni S (2002) Phys Chem Chem Phys 4: 5697
40. Towens CH, Dailey BP (1949) J Chem Phys 17: 782
41. Code RF, Ramsey NF (1971) Phys Rev A 4: 1945
42. Reid (Jr) RV, Vaida ML (1973) Phys Rev A 7: 1841
43. Bishop DM, Cheung LM (1979) Phys Rev A 20: 381
44. Zamani-Khamiri O, Hameka HF (1981) J Chem Phys 75: 781
45. Kim H, Hameka HF, Zeroka D (1988) J Chem Phys 88: 3159
46. Bishop DM, Cybulski SM (1994) J Chem Phys 100: 6628
47. Becke AD (1993) J Chem Phys 98: 5648
48. Becke AD (1988) Phys Rev A 38: 3098
49. Lee C, Yang W, Parr RG (1988) Phys Rev B 37: 785
50. Perdew JP, Burke K, Ernzerhof M
51. (1996) Phys Rev Lett 77: 3865
52. (1997) ibiden 78: 1396
53. Burke K, Perdew JP, Wang Y, Dobson JF (ed), Vignale G. (ed), and Das M. P. (ed) (1988) Electronic density functional theory: recent progress and new dimensions, Plenum, New York
54. Frisch MJ, Trucks GW, Schlegel HB, Scuseria GE, Robb MA, Cheeseman JR, Montgomery JA (Jr), Vreven T, Kudin KN, Burant JC, Millam JM, Iyengar SS, Tomasi J, Barone V, Mennucci B, Cossi M, Scalmani G, Rega N, Petersson GA, Nakatsuji H, Hada M, Ehara M, Toyota K, Fukuda R, Hasegawa J, Ishida M, Nakajima T, Honda Y, Kitao O, Nakai H, Klene M, Li X, Knox JE, Hratchian HP, Cross JB, Bakken V, Adamo C, Jaramillo J, Gomperts R, Stratmann RE, Yazyev O, Austin AJ, Cammi R, Pomelli C, Ochterski JW, Ayala PY, Morokuma K, Voth GA, Salvador P, Dannenberg JJ, Zakrzewski VG, Dapprich S, Daniels AD, Strain MC, Farkas O, Malick DK, Rabuck AD, Raghavachari K, Foresman JB, Ortiz JV, Cui Q, Baboul AG, Clifford S, Cioslowski J, Stefanov BB, Liu G, Liashenko A, Piskorz P, Komaromi I, Martin RL, Fox DJ, Keith T, Al-Laham MA, Peng CY, Nanayakkara A, Challacombe M, Gill PMW, Johnson B, Chen W, Wong MW, Gonzalez C, Pople JA (2003) Gaussian 03, Revision B.05 (Gaussian, Inc., Wallingford CT)
55. Antony J, Hansen B, Hemmingsen L, Bauer R (2000) J Phys Chem A 104: 6047
56. Cummins PG, Dunmur DA (1973) J Phys D: Appl Phys 7: 451
57. Mathieson McLA, Montheath Robertson J, Sinclair VC (1950) Acta Cryst 3: 245
58. Montheath Robertson J (1958) Rev Mod Phys 30: 155
59. Pratt Brock C, Dunitz JD (1990) Acta Cryst 46: 795